

Semiconductor-semiconductor transition in $\text{Mg}[\text{Ti}_2]\text{O}_4$

H. D. Zhou and J. B. Goodenough

Texas Materials Institute, ETC 9.102, The University of Texas at Austin, 1 University Station, C2201, Austin, Texas 78712, USA

(Received 28 February 2005; published 14 July 2005)

Preparation of a nearly stoichiometric $\text{Mg}[\text{Ti}_2]\text{O}_4$ spinel with a transition at $T_t=260$ K has been accomplished by solid-state reaction. Schmidt *et al.* [Phys. Rev. Lett. **92**, 056402, 2004] have shown a tetragonal ($c/a < 1$)-cubic transition at $T_t=260$ K with the formation of long-range ordering of Ti–Ti dimers. We report transport measurements on cold-pressed samples that show a p -type thermoelectric power $\alpha(T)$ above T_t that drops sharply on cooling below T_t to become n -type below 170 K. The p -type conductivity requires a correlation splitting of the $\text{Ti}^{4+}/\text{Ti}^{3+}$ and $\text{Ti}^{3+}/\text{Ti}^{2+}$ redox couples and a ratio $\text{Mg}/\text{Ti} \neq 1/2$ to introduce holes into the $\text{Ti}^{4+}/\text{Ti}^{3+}$ couple. Above T_t , holes are increasingly trapped out at acceptor sites as the temperature is lowered; below T_t , the holes occupy one-electron dimers that may act as mobile p -type polarons or as donors to create three-electron dimers that act as n -type polarons. The transition at T_t is, therefore, a semiconductor-semiconductor transition Ti–Ti associated with dimerization instabilities. The dimerization is caused by lattice instabilities resulting from a double-well Ti–Ti bond potential at a crossover from localized to itinerant electronic behavior. The spin-1/2 odd-electron dimers give a Curie component to the magnetic susceptibility; this component is not due to impurities. A drop in $\chi(T)$ on cooling through T_t reflects formation of spin-paired dimers, but short-range dimer fluctuations also reduce $\chi(T)$ in an extended temperature range above T_t . With increasing x in $\text{Mg}[\text{Mg}_x\text{Ti}_{2-x}]\text{O}_4$, the introduction of Mg^{2+} and Ti^{4+} ions on the octahedral sites disrupts long-range ordering of dimers, and the temperature interval of the transition is broadened and lowered. Although evidence for the transition is washed out in the $\rho(T)$ and $\chi(T)$ data for $x \geq 0.24$, the $\alpha(T)$ and low-temperature $\chi(T)$ data show the formation of disordered Ti–Ti dimers for all $x < 0.3$.

DOI: [10.1103/PhysRevB.72.045118](https://doi.org/10.1103/PhysRevB.72.045118)

PACS number(s): 71.30.+h, 72.20.Pa, 72.80.Ga, 75.30.Cr

I. INTRODUCTION

The normal spinels $\text{A}[\text{B}_2]\text{O}_4$ having a main-group A^{2+} ion on the tetrahedral sites and $\text{B}=\text{Ti}$ or V on the octahedral sites are of interest because the dominant d -electron interactions (i.e., the Ti–Ti or V–V interactions across shared octahedral-site edges) are near the crossover from localized to itinerant electronic behavior. An early search¹ for a transition from localized to itinerant electronic behavior in the $\text{A}[\text{V}_2]\text{O}_4$ spinels was frustrated by an inability to get a small enough A^{2+} cation (Be^{2+} was not considered); a crossover from polaronic to metallic behavior was only found in the mixed-valent system $\text{A}_{1-x}\text{Li}_x[\text{V}_2]\text{O}_4$. Interest in the titanium spinels was first sparked by the discovery by Johnston *et al.*² of superconductivity with a $T_C=11$ K in the mixed-valent compound $\text{Li}[\text{Ti}_2]\text{O}_4$. A natural extension of this finding was to investigate whether the single-valent compound $\text{Mg}[\text{Ti}_2]\text{O}_4$ is metallic, a magnetic semiconductor, or at the crossover from metallic to localized electronic behavior.

An initial investigation³ of the electrical and magnetic properties of polycrystalline samples of nominal $\text{Mg}[\text{Mg}_x\text{Ti}_{2-x}]\text{O}_4$ was a search for evidence of superconductivity in this system; none was found, but an increase in the electrical conductivity with increasing x was noted.

In a more careful study, Isobe and Ueda⁴ found a tetragonal ($c/a < 1$) to cubic transition at $T_t \approx 250$ K in nearly stoichiometric $\text{Mg}[\text{Ti}_2]\text{O}_4$. The resistivity below T_t was semiconductive; above T_t , the resistivity of their polycrystalline sample appeared to become metallic. A sharp decrease in the magnetic susceptibility on cooling through T_t led these authors to assume the transition involved the formation of

Ti–Ti spin-singlet dimers, and Schmidt *et al.*⁵ confirmed an ordering of dimers below T_t in a helical configuration about the c axis. However, whether this transition marks a Peierls semiconductor-metal transition, as has been assumed, or a semiconductor-semiconductor transition associated with a lattice instability as the Mott-Hubbard transition is approached from the itinerant-electron side remains an open question.

Exploration of this question hinges on the ability to prepare oxygen-stoichiometric $\text{Mg}[\text{Ti}_2]\text{O}_4$. Sugimoto *et al.*⁶ and Isobe and Ueda⁷ have emphasized problems associated with the volatility of MgO at the sintering temperatures and of the preparation of an essentially stoichiometric, single-phase $\text{Mg}[\text{Ti}_2]\text{O}_4$ spinel. We used a cold-pressing technique to densify our polycrystalline samples in order to obtain meaningful resistivity $\rho(T)$ data. Our data show a semiconductor-semiconductor transition similar to that found in layered LiVO_2 in which V_3 trimers are formed below a T_t in a close-packed plane of edge-shared $\text{VO}_{6/3}$ octahedra.⁸

II. EXPERIMENT

Polycrystalline samples of $\text{Mg}[\text{Mg}_x\text{Ti}_{2-x}]\text{O}_4$ spinels were prepared by solid-state reaction. Mixtures of appropriate molar ratios of MgO , Ti metal, and Ti_2O_3 were ground together for each composition, placed into a molybdenum crucible, and put into a silica tube that was then evacuated to $\sim 10^{-6}$ torr before firing at 1080 °C for 6 h. The fired product was reground, cold pressed into pellets, and fired for another 6 h in an evacuated tube as before.

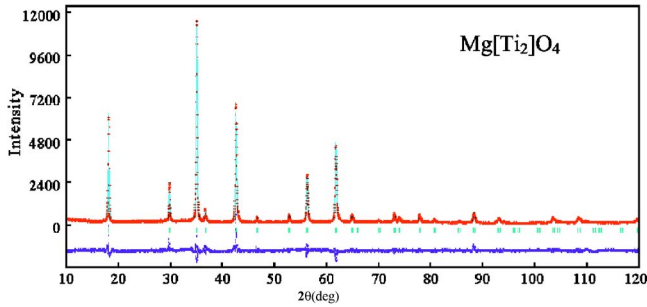


FIG. 1. (Color online) X-ray-diffraction pattern of $\text{Mg}[\text{Ti}_2]\text{O}_4$. The bottom curve is the difference between the experimental data and the refinement. The vertical bars indicate the Bragg peak positions.

Powder x-ray-diffraction (XRD) patterns were recorded with a Philips 1729 diffractometer equipped with a pyrolytic graphite monochromator and $\text{CuK}\alpha$ radiation (1.54059 \AA). Data were collected in steps of 0.020° over the range $10^\circ \leq 2\theta \leq 120^\circ$ with a count time of 20 s per step. Peak profiles for the XRD data were fitted with the program Rietan 2000. Refinements gave R_{WP} values of about 10% for all samples.

Magnetic measurements were made on warming in a measuring field $H=1 \text{ kOe}$ after cooling in zero field (ZFC) with a Quantum Design dc SQUID magnetometer.

The thermoelectric power $\alpha(T)$ was obtained with a laboratory-built apparatus as described elsewhere;⁹ the resistivity $\rho(T)$ was measured with a four-probe technique on cold-pressed samples. The cold-pressing technique is described elsewhere.¹⁰ The $\alpha(T)$ and $\rho(T)$ data were obtained in a vacuum of 10^{-5} torr.

III. RESULTS

Earlier studies^{6,7} have highlighted the two major problems to be overcome for making stoichiometric, single-phase $\text{Mg}[\text{Ti}_2]\text{O}_4$. Volatilization of MgO at the sintering temperature can be compensated by the addition of extra MgO appropriate to a given firing temperature and duration. The oxidation of Ti^{3+} to Ti^{4+} , which occurs even in an evacuated atmosphere, can be avoided by starting with reduced precursors. We prepared a stoichiometric $\text{Mg}[\text{Ti}_2]\text{O}_4$ from $\text{Mg}_{1+y}\text{Ti}_2\text{O}_{4-\delta}$ ($y \approx 0.1$, $\delta \approx 0.2$) by carefully selecting a firing temperature of 1080°C for a time of 12 h. Our product was single-phase $\text{Mg}[\text{Ti}_2]\text{O}_4$ to XRD with no trace of the commonly reported corundum impurity $\text{MgTiO}_3\text{-Ti}_2\text{O}_3$. The room-temperature cubic lattice parameter for our $\text{Mg}[\text{Ti}_2]\text{O}_4$, as calculated by Rietan 2000 with $R_{\text{WP}}=9.55\%$, was $a=8.51000(10) \text{ \AA}$, which is larger than the $a=8.506$ and 8.505 \AA values reported by Refs. 6 and 7, respectively. Figure 1 shows the XRD pattern and its Rietan 2000 refinement for our $\text{Mg}[\text{Ti}_2]\text{O}_4$.

Since the $\text{Mg}[\text{Mg}_x\text{Ti}_{2-x}]\text{O}_4$ ($0 \leq x \leq 1$) system has been shown¹¹ to obey Vegard's law and the lattice parameter for $\text{Mg}[\text{MgTi}]\text{O}_4$ is $a=8.4409 \text{ \AA}$, we estimate the value of x from the expression

$$x = 1 - (a - 8.4409)/0.0691 \quad (1)$$

on the assumption that our $a=8.5100 \text{ \AA}$ corresponds to the stoichiometric $\text{Mg}[\text{Ti}_2]\text{O}_4$. According to Eq. (1), the nominal

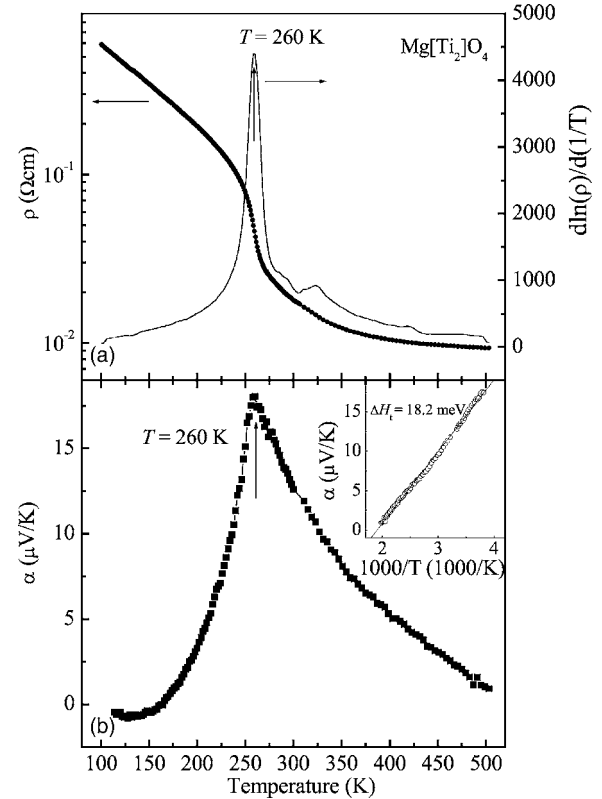


FIG. 2. Temperature dependencies of (a) resistivity $\rho(T)$ and $d(\ln \rho)/d(1/T)$, (b) thermoelectric power $\alpha(T)$ for $\text{Mg}[\text{Ti}_2]\text{O}_4$. Inset of (b): $\alpha \sim 1/T$ curve with $T > 260 \text{ K}$.

$\text{Mg}[\text{Ti}_2]\text{O}_4$ samples reported to have an $a=8.505 \text{ \AA}$ correspond to $\text{Mg}[\text{Mg}_{0.07}\text{Ti}_{1.93}]\text{O}_4$, which introduces 0.07 Ti^{4+} /formula unit. We use Eq. (1) to estimate the value of x in our $\text{Mg}[\text{Mg}_x\text{Ti}_{2-x}]\text{O}_4$ samples.

Figure 2 shows the temperature dependencies of the resistivity $\rho(T)$ and the thermoelectric power $\alpha(T)$ over the interval $100 \text{ K} < T < 500 \text{ K}$ for $\text{Mg}[\text{Ti}_2]\text{O}_4$. The resistivity shows a semiconductor-semiconductor transition at $T_i \approx 260 \text{ K}$. A similar $T_i=260 \text{ K}$ was reported by Schmidt *et al.*⁵ for the tetragonal-cubic structural transition. At 500 K , $\rho(T)$ falls to as low as $10^{-2} \Omega \text{ cm}$, and the jump on cooling through T_i is initiated at about 270 K . Since $\rho \sim \exp(-E_a/kT)$ describes semiconductive behavior, we plot $d(\ln \rho)/d(1/T)$ to show how the effective activation energy evolves with temperature. This plot shows a sharp peak at $T_i=260 \text{ K}$. In Fig. 2(b), an $\alpha(T) > 0$ shows the onset of a sharp drop on cooling through T_i , $\alpha(T)$ becoming weakly negative below about 170 K . Above T_i , the increase in $\alpha(T) > 0$ on cooling signals a trapping out of mobile holes, and an $\alpha(T) \sim \Delta H_i/2kT$ at $T > T_i$ gives a trapping enthalpy $\Delta H_i=18.2 \text{ meV}$.

Figure 3 shows the paramagnetic susceptibility $\chi(T)$ of $\text{Mg}[\text{Ti}_2]\text{O}_4$ below room temperature. As reported by others, $\chi(T)$ drops sharply on cooling through T_i from a nearly temperature-independent value in the short interval $T_i < T < 300 \text{ K}$. The sharp maximum in $d\chi/dT$ at $T_i=260 \text{ K}$ has an onset temperature of about 270 K on cooling. Below 150 K , the increase in $\chi(T)$ can be described by a Curie law

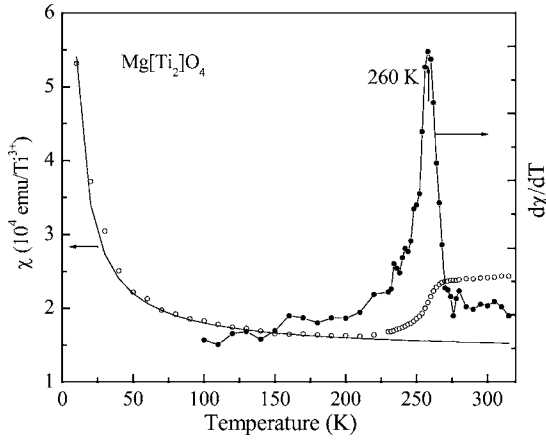


FIG. 3. Molar magnetic susceptibility $\chi(T)$ and its $d\chi/dT$ vs T curve for $\text{Mg}[\text{Ti}_2]\text{O}_4$. The solid line is the fit from the equation $\chi = \chi_0 + C/T$ with $\chi_0 = 0.00014 \text{ emu}/\text{Ti}^{3+}$ and $C = 0.004 \text{ emuK}/\text{Ti}^{3+}$.

$$\chi - \chi_0 = C/T \quad (2)$$

where $\chi_0 = 0.00014 \text{ emu}/\text{Ti}$ and $C = 0.004 \text{ emuK}/\text{Ti}$. From Eq. (2), we estimate there are about 0.01 localized spins $S = 1/2$ per Ti atom associated with nonstoichiometry or defects, not an impurity phase.

Figures 4–6 show, respectively, the $\rho(T)$, $\alpha(T)$, and $\chi(T)$ curves for $\text{Mg}[\text{Mg}_x\text{Ti}_{2-x}]\text{O}_4$ samples with different values of x . As x increases, the step in $\rho(T)$ broadens, becoming washed out for $x \geq 0.24$. Although $\rho(T)$ increases with x at $T > T_i$, its behavior below T_i shows a more complex evolution with x . The $\alpha(T)$ curves, on the other hand, show that the decrease in T_i and broadening of the transition is retained to $x = 0.29$. The magnetic susceptibility $\chi(T)$ shows a progressive increase below room temperature in the temperature-independent component χ_0 that masks any evi-

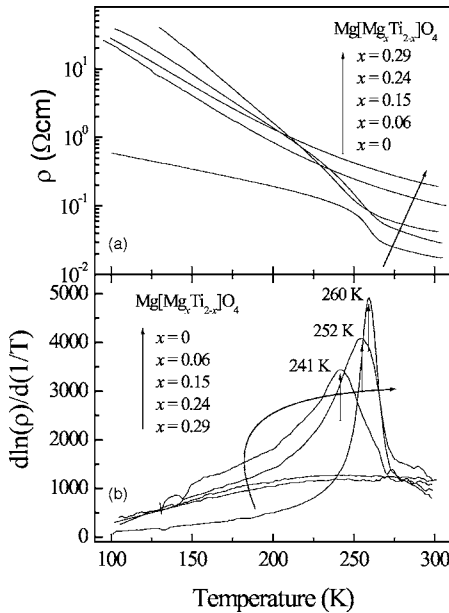


FIG. 4. Temperature dependencies of (a) resistivity $\rho(T)$ and (b) $d(\ln \rho)/d(1/T)$ for $\text{Mg}[\text{Mg}_x\text{Ti}_{2-x}]\text{O}_4$.

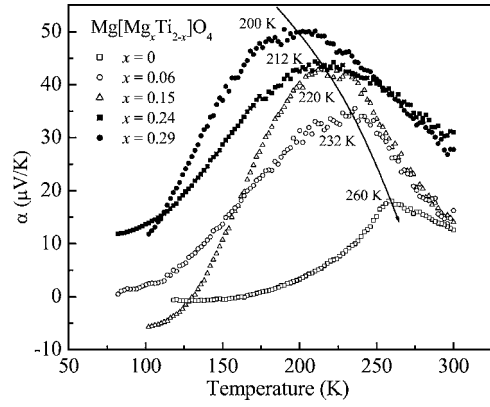


FIG. 5. Temperature dependencies of thermoelectric power $\alpha(T)$ for $\text{Mg}[\text{Mg}_x\text{Ti}_{2-x}]\text{O}_4$.

dence of a transition at $x \geq 0.24$, but the localized-spin component that manifest itself at lower temperatures is retained.

IV. DISCUSSION

Figure 4 shows that the transition temperature T_i and the sharpness of the transition at T_i both increase as x decreases in the spinels $\text{Mg}[\text{Mg}_x\text{Ti}_{2-x}]\text{O}_4$, i.e., as the ratio $\text{Ti}^{4+}/\text{Ti}^{3+}$ decreases. It is therefore noteworthy that the $T_i = 260 \text{ K}$ found in our samples is higher than that reported by others with the exception of the sample of Schmidt *et al.*⁵, which also had a $T_i = 260 \text{ K}$. The neutron-diffraction data showing the long-range ordering of Ti–Ti dimers below T_i in their sample signal that a $T_i = 260 \text{ K}$ is a signature of a nearly stoichiometric $\text{Mg}[\text{Ti}_2]\text{O}_4$. Nevertheless, the high-temperature thermoelectric power $\alpha(T)$ of Fig. 2 shows a p -type conduction, which requires conduction in a band that is more than half filled. Although the local trigonal crystal-line field at the octahedral sites of a spinel may stabilize from the threefold-degenerate t_{2g} -orbital manifold of the octahedral-site Ti^{3+} ions a nondegenerate a_1 orbital oriented along one of the $\langle 111 \rangle$ axes, this band would be half filled were all the Ti ions trivalent, since the only way to reduce

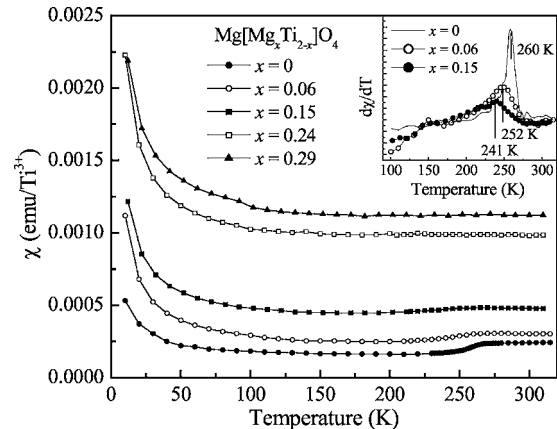


FIG. 6. Molar magnetic susceptibility $\chi(T)$ for $\text{Mg}[\text{Mg}_x\text{Ti}_{2-x}]\text{O}_4$. Inset: $d\chi/dT$ vs T curves for $x = 0, 0.06,$ and 0.15 samples.

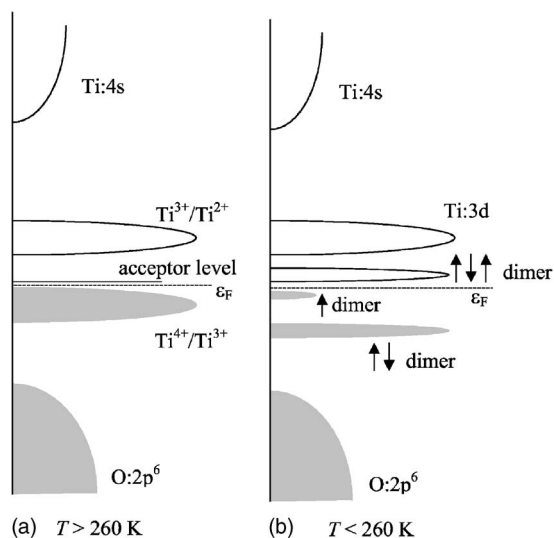


FIG. 7. Schematic energy diagrams for $\text{Mg}_{1-\delta}[\text{Ti}_2]\text{O}_4$ with (a) $T > 260$ K and (b) $T < 260$ K. The arrows distinguish two-, one-, and three-electron dimers.

the $[\text{Ti}_2]\text{O}_4$ array to make this band more than half filled would be to introduce interstitial octahedral-site Ti atoms, which is highly improbable. We are therefore forced to conclude that an on-site electron-electron electrostatic energy splits the $\text{Ti}^{4+}/\text{Ti}^{3+}$ and $\text{Ti}^{3+}/\text{Ti}^{2+}$ redox couples as indicated schematically in Fig. 7(a).

There are two mechanisms by which holes may be introduced into the $\text{Ti}^{4+}/\text{Ti}^{3+}$ couple; each of these requires a ratio $\text{Mg}/\text{Ti} \neq 1/2$. A Mg vacancy on the tetrahedral sites would introduce two Ti^{4+} ions into a $[\text{Ti}_2]\text{O}_4$ array; an octahedral-site Mg^{2+} ion would be charge compensated by a Ti^{4+} ion in a $[\text{Mg}_x\text{Ti}_{2-x}]\text{O}_4$ array. Given the empirical route by which the correct amount of extra Mg is introduced into the starting synthetic mix, it is impossible to control the Mg/Ti ratio precisely at 1/2 in the final product, so the introduction of some Ti^{4+} into a correlation-stabilized $\text{Ti}^{4+}/\text{Ti}^{3+}$ redox couple is inevitable. The qualitative arguments to follow do not depend on which doping mechanism is applicable.

The $\rho(T)$ data of Fig. 2 show that the transition at T_t is a semiconductor-semiconductor transition, which means it is not a classical insulator-metal Peierls transition. The high-temperature phase may be a polaronic conductor typical of a strongly correlated system or it may contain itinerant holes that become trapped. It is not possible to determine the size of any polarons from the $\alpha(T)$ data since the concentration of mobile holes is not known and, with lowering temperature, there is a continuous trapping out of the holes at acceptor sites neighboring the dopant that introduced them, i.e., the Mg vacancies on tetrahedral sites, $\text{Mg}_{1-\delta}[\text{Ti}_2]\text{O}_4$, or the excess Mg on octahedral sites, $\text{Mg}[\text{Mg}_x\text{Ti}_{2-x}]\text{O}_4$. A high-temperature activation energy $E_a = \Delta H_m + \Delta H_t/2 = 15$ meV obtained from $d(\ln \rho)/d(1/T)$ and a $\Delta H_t \approx 18$ meV from Fig. 2 gives a polaron motional enthalpy $\Delta H_m \approx 6$ meV, which is too small for small-polaron behavior. The $\rho(T) \rightarrow 10^{-2} \Omega \text{ cm}$ at higher temperatures and a small ΔH_m are characteristic of a narrow band at the crossover from itinerant

to localized electronic behavior where the appearance of a double-well bond potential introduces lattice instabilities. In this case, the double-well potential is associated with the Ti–Ti bonding across shared octahedral-site edges. The double-well bond potential manifests itself at lower temperatures in the formation of localized molecular orbitals in spin-paired Ti–Ti dimers that interact only weakly with one another across longer Ti–Ti bonds. Since long-range dimer ordering is difficult to achieve in the $[\text{B}_2]\text{O}_4$ spinel framework, the lattice instabilities manifest themselves over an extended temperature range above T_t as dimer fluctuations, i.e., as short-range antiferromagnetic fluctuations that increase in concentration as the temperature T_t . These fluctuations reduce the magnetization M induced by an applied magnetic field H , thereby reducing $\chi = M/H$ and increasing $1/\chi$ to give a nearly temperature-independent $\chi(T)$ in the short 60 K temperature interval above T_t in Fig. 3; the nearly temperature-independent $\chi(T)$ above T_t does not necessarily signal a Pauli paramagnetism associated with a metallic band.

The sharp drop in $\alpha(T)$ on cooling through T_t signals the introduction of electron donors. Long-range ordering of Ti–Ti dimers below T_t condenses the $\text{Ti}^{4+}/\text{Ti}^{3+}$ redox couple into two-electron dimer states and traps holes into one-electron $\text{Ti}^{3+}/\text{Ti}^{4+}$ dimers; the electrons in these spin-1/2 dimers would be less stable than those in the spin-paired dimers; these dimers would correspond to small-polaron holes free to hop between dimers, but they would also act as donors that create three-electron spin-1/2 dimers that hop as electronic polarons to give n -type conduction. Since the energy separation between one- and three-electron dimers would be smaller than that between the two- and one-electron dimers, the mobility of the electronic polarons would be higher than the mobility of the polaronic holes at low temperature. We believe this is the reason $\alpha(T)$ drops to a negative value below 170 K.

The concentration of spin-1/2 dimers does not change with temperature below T_t , and whether mobile or stationary, n - or p -type, they would contribute to the low-temperature Curie susceptibility of Eq. (2).

With increasing x in the system $\text{Mg}[\text{Mg}_x\text{Ti}_{2-x}]\text{O}_4$, the introduction of Mg^{2+} and Ti^{4+} ions on the octahedral sites disrupts long-range, cooperative ordering of the Ti–Ti dimers. Nevertheless, the $\alpha(T)$ data of Fig. 5 show that there is a transition from dimer fluctuations to static dimer formation on lowering the temperature; but the lack of cooperative long-range ordering lowers and broadens the temperature interval over which the transition to static dimers occurs. Moreover, the introduction of Mg ions onto the octahedral sites also disrupts the periodic potential so as to transform any itinerant character of the strongly correlated electrons above T_t toward a more localized small-polaron behavior of larger motional enthalpy. The mobility of the holes above T_t is thereby reduced, and a concomitant increase in the trapping enthalpy reduces the concentration of mobile holes at a given temperature. Therefore, the systematic increase with x in $\rho(T)$ above T_t is to be expected. Below T_t , on the other hand, the lack of long-range dimer order makes any qualitative discussion of the more complex evolution of $\rho(T)$ with x too speculative.

V. CONCLUSIONS

A nearly stoichiometric, single-phase sample of $\text{Mg}[\text{Ti}_2]\text{O}_4$ spinel has been successfully prepared by solid-state reaction, but the volatility of Mg at the sintering temperature made it impossible to control precisely the Mg/Ti ratio to 1/2. A transition temperature $T_t=260$ K was like that of Schmidt *et al.*,⁵ who identified a long-range ordering of Ti–Ti dimers below T_t ; it is the highest value of T_t that has been reported. Nevertheless, a *p*-type conductivity above T_t signals that strong correlations split the $\text{Ti}^{4+}/\text{Ti}^{3+}$ and $\text{Ti}^{3+}/\text{Ti}^{2+}$ couples and that a ratio $\text{Mg}/\text{Ti} \neq 1/2$ introduces holes into the $\text{Ti}^{4+}/\text{Ti}^{3+}$ couple. Accordingly, the transition at T_t was shown to be a semiconductor-semiconductor transition and not an insulator-metal transition associated with a classic Peierls distortion. Rather, a double-well Ti–Ti bond potential introduces lattice instabilities as the transition from itinerant to localized electronic behavior is approached from the itinerant-electron side.

Above T_t , polaronic holes become increasingly trapped at acceptor sites with decreasing temperature; but below T_t , the holes are trapped in one-electron spin-1/2 dimers, which may act as polaronic holes that hop between dimers or as

donors to two-electron dimers to make spin-1/2 three-electron dimers and undimerized Ti^{4+} -ion pairs. The concentration of spin-1/2 dimers remains unchanged in both of these processes, and it gives rise to a Curie component in the magnetic susceptibility that manifests itself at lower temperatures. The formation of three-electron dimers is energetically favored over transfer of an electron from a two-electron dimer to a one-electron dimer, so $\alpha(T)$ becomes negative below 170 K.

The introduction of Mg into the octahedral sites in $\text{Mg}[\text{Mg}_x\text{Ti}_{2-x}]\text{O}_4$ disrupts long-range ordering of the dimers, but a transition from dimer fluctuations to static, randomly ordered dimers occurs over a lower and broader temperature interval. Although the transition appears to be washed out for $x \geq 0.24$ in the $\rho(T)$ and $\chi(T)$ curves, the thermoelectric-power and low-temperature $\chi(T)$ data show that Ti–Ti dimer formation, though increasingly more random, occurs for all $x < 0.3$.

ACKNOWLEDGMENTS

The authors thank the NSF and the Robert A. Welch Foundation of Houston, TX, for financial support.

¹D. B. Rogers, R. J. Arnott, A. Wold, and J. B. Goodenough, *J. Phys. Chem. Solids* **24**, 347 (1963).

²D. C. Johnston, H. Prakash, W. H. Zachariesen, and R. Viswanathan, *Mater. Res. Bull.* **8**, 777 (1973).

³H. Hohl, C. Kloc, and E. Bucher, *J. Solid State Chem.* **125**, 216 (1996).

⁴M. Isobe and Y. Ueda, *J. Phys. Soc. Jpn.* **71**, 1848 (2002).

⁵M. Schmidt, W. Ratcliff II, P. G. Radaelli, K. Refson, N. M. Harrison, and S. W. Cheong, *Phys. Rev. Lett.* **92**, 056402 (2004).

⁶W. Sugimoto, N. Kaneko, Y. Sugahara, and K. Kuroda, *J. Ceram. Soc. Jpn.* **105**, 101 (1997).

⁷M. Isobe and Y. Ueda, *J. Alloys Compd.* **383**, 85 (2004).

⁸P. F. Bongers, Thesis, University of Leiden (unpublished).

⁹J. B. Goodenough, J.-S. Zhou, and J. Chan, *Phys. Rev. B* **47**, 5275 (1993).

¹⁰J.-S. Zhou, J. B. Goodenough, and B. Dabrowski, *Phys. Rev. B* **67**, 020404(R) (2003).

¹¹A. Feltz and M. Steinbrück, *J. Less-Common Met.* **167**, 233 (1991).